Phys. Status Solidi A **211**, No. 1, 191–194 (2014) / **DOI** 10.1002/pssa.201330060

physica status solidi a
www.pss-a.com
applications and materials science

The physical nature of bipolar resistive switching in Pt/$BiFe_{0.95}Mn_{0.05}O_3$/Pt memory devices

J. M. Luo*[,1,2], R. Q. Chen[3], and S. P. Lin[,2,4]**

[1] School of Physics and Optical Information Sciences, Jiaying University, Meizhou, Guangdong 514015, P. R. China
[2] State Key Laboratory of Optoelectronic Materials and Technologies, Sun Yat-Sen University, Guangzhou 510275, P. R. China
[3] Center of Experimental Teaching for Common Basic Courses, South China Agricultural University, Guangzhou 510642, P. R. China
[4] Sino-French Institute of Nuclear Engineering and Technology, Zhuhai Campus, Sun Yat-sen University, Zhuhai 519082, P. R. China

Received 17 June 2013, revised 25 September 2013, accepted 25 September 2013
Published online 31 October 2013

Keywords $Bi(Fe,Mn)O_3$, compliance current, memory devices, resistive switching

* Corresponding author: e-mail zsuljm@163.com, Phone: +86 0753 2186808, Fax: +86 0753 2354179
** e-mail lshpeng@mail.sysu.edu.cn, Phone: +86 020 84113390, Fax: +86 020 84113390

www.spm.com.cn

Pt/$BiFe_{0.95}Mn_{0.05}O_3$/Pt memory devices show stable bipolar resistive switching characteristics with a resistance ratio of about 10 and a retention time of more than 10^3 s. Based on the analysis of current conduction, oxygen vacancies are supposed to play an important role in the formation of conducting path, and the temperature dependence of the resistance in the low-resistive state demonstrates that the resistance increases with temperature slightly. Additionally, on increasing the compliance current during the SET process, the resistance in the low-resistive state decreases while the RESET current increases. However, the RESET voltage is observed to be independent of the compliance current. These results can be explained by the conductive filament mechanism originating from the trapping and detrapping of electrons.

© 2013 WILEY-VCH Verlag GmbH & Co. KGaA, Weinheim

1 Introduction Multiferroic bismuth ferrite (BFO) has attracted a tremendous flurry of research interest for its promising potential in novel multifunctional device applications [1–5]. BFO is reported to possess remarkable properties including ferroelectricity and antiferromagnetism with a high Curie temperature (T_C) [6], a high Néel temperature (T_N) [7], and a large remnant polarization ($\sim 100\,\mu C\,cm^{-2}$) [8]. However, the large leakage current originating from the presence of Fe^{2+} and oxygen vacancies (OVs) markedly deteriorates the multiferroic performance and limits its scalability [9]. In order to reduce the leakage current and modify the multiferroic properties, many studies have been focused on the metal-ion site engineering. Bi-site substitution can control the volatile Bi atoms and suppress the formation of OVs, such as La [10]; Fe-site substitution by high-valence ions can decrease the OVs and suppress the formation of Fe^{2+} due to charge compensation, such as Mn [11].

Most recently, BFO-based thin films are considered to be promising candidates for future resistive random access memories (RRAMs) because of their resistive switching (RS) characteristics [12–17]. To explain this RS behavior, two main mechanisms have been proposed. One type is the interface-barrier model, in which the RS originates from the modulation of a Schottky barrier, owing to the trapping and detrapping of carriers [12] or the migration of OVs [13, 14] at the interface. Another type is the conductive-filament model, in which the RS results from the formation and rupture of a filamentary conducting path, due to the migration and connection of OVs in thin films [15–17]. Thus, the study of the RS mechanism in BFO-based thin films is still a controversial issue.

The nonpolar resistive switching in Mn-doped BFO thin films has been reported previously [18], and can be attributed to a valence variation effect between Fe^{3+} and Fe^{2+} due to the neutralization and ionization of OVs. In this study, further investigation on the physical nature of stable bipolar resistive switching (BRS) has been carried out in Pt/$BiFe_{0.95}Mn_{0.05}O_3$ (BFMO)/Pt memory devices. Based on the analysis of temperature and compliance current effects on the BRS

© 2013 WILEY-VCH Verlag GmbH & Co. KGaA, Weinheim

characteristics, a better understanding of the conductive filament mechanism in BFMO thin films can be achieved.

2 Experimental $BiFe_{0.95}Mn_{0.05}O_3$ thin films were fabricated by depositing a sol–gel chemical solution on Pt/Ti/SiO_2/Si substrates. $Bi(NO_3)_3 \cdot 5H_2O$, $Fe(NO_3)_3 \cdot 9H_2O$, and $C_6H_9MnO_6 \cdot 2H_2O$ were used to prepare the precursor solutions. The BFMO solutions of 0.2 mol/L concentration (Toshima MFG Co. Ltd.) were spin coated at 3000 rpm for 30 s, and then dried at 350 °C for 5 min. This procedure was repeated several times until the desired thickness of about 350 nm was attained, and finally the films were annealed at 500 °C in air for 30 min. The film structure was examined by X-ray diffraction (XRD, D-MAX 2200VPC), the chemical state of Mn ions was analyzed by X-ray photoelectron spectroscopy (XPS, ESCALAB 250), and the surface morphology of the film was characterized by a scanning probe microscope (SPM, CSPM5500). After Pt top electrode deposition on the film with a diameter of 0.3 mm, the current–voltage characteristics were studied using a Keithley 4200-SCS semiconductor parameter analyzer.

3 Results and discussions The XRD patterns of a BFMO thin film annealed at 500 °C are shown in Fig. 1a, and the inset of Fig. 1a demonstrates the Mn doping by the XPS spectra of Mn 2p. The diffraction peaks are well indexed according to the BFO phase, suggesting that the thin film with a perovskite structure is well grown on Pt substrate and no impurity phase is detected. Figure 1b shows the corresponding surface morphology in the SPM image with a scanning area of $1.78 \times 1.78\ \mu m^2$. The root-mean-square roughness is measured to be about 2.51 nm, and a good crystalline quality can be observed in the BFMO polycrystalline film.

The initial forming process with a high forming voltage of about 7 V is shown in the inset of Fig. 2a, after which BRS characteristics of BFMO thin film for different compliance currents are investigated. The typical current–voltage behavior for a compliance current of 5 mA has been selected, as described in Fig. 2a, where the arrows represent the voltage sweep direction. When the bias is swept in the positive direction, a "SET" process occurs at a certain threshold voltage where the current suddenly increases, and the device shifts from the high-resistive state (HRS) to the low-resistive state (LRS). When the bias is swept in the negative direction, a "RESET" process takes place at an appropriate voltage where the current drops abruptly, and the device switches back to the HRS. Figure 2b shows the

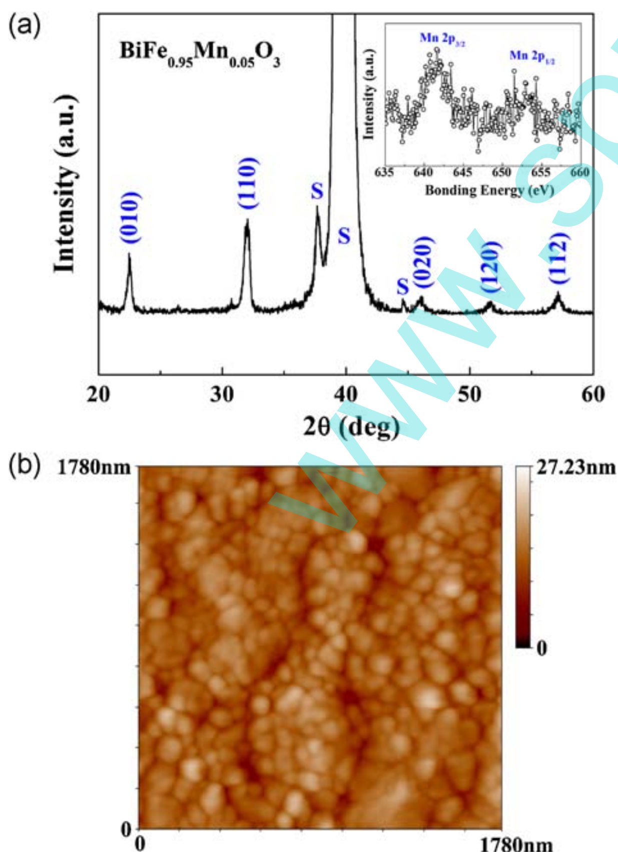

Figure 1 (a) XRD patterns and (b) SPM image of BFMO thin film. The inset of (a) shows the XPS spectra of Mn 2p, and the substrate peaks are marked with S.

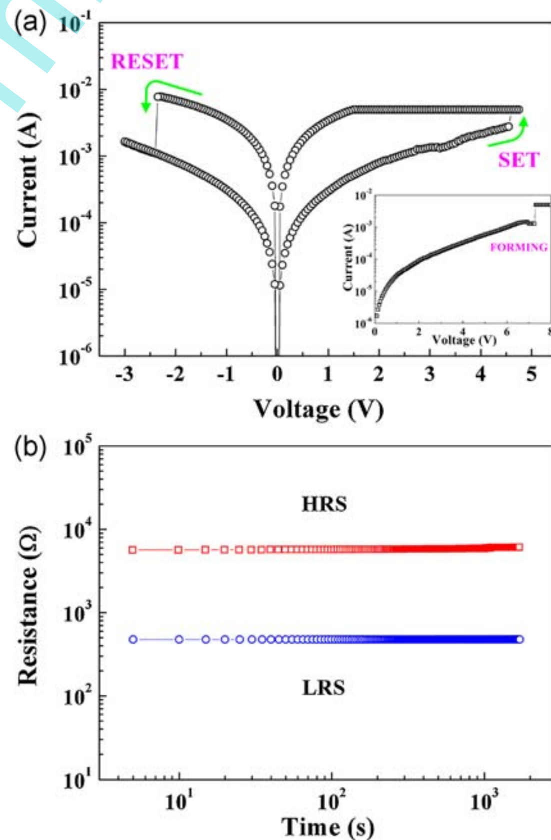

Figure 2 BRS characteristics in Pt/BFMO/Pt memory devices. (a) Current–voltage curves plotted in semi-log scale. The inset shows the forming process. (b) Retention of the HRS and LRS with a read voltage of 0.1 V.

www.spm.com.cn

© 2013 WILEY-VCH Verlag GmbH & Co. KGaA, Weinheim

retention characteristic of Pt/BFMO/Pt memory devices. The resistance ratio of HRS to LRS is measured to be more than 10 at a read voltage of 0.1 V, and no significant changes in the resistance of either HRS or LRS for 2×10^3 s can be observed at room temperature, which is indicative of a nonvolatile and stable BRS property.

The charge-transport mechanisms have been studied by analyzing the current–voltage curves, which are replotted on the double-logarithmic scale in Fig. 3a for the positive voltage range and Fig. 3b for the negative voltage range, respectively. In HRS, a trap-limited space-charge-limited current (TL-SCLC) conduction with an exponentially distributed trap can be observed [19],

$$J = N_c \mu e \left(\frac{\varepsilon_r \varepsilon_0}{e N_t}\right)^l \left(\frac{l}{l+1}\right)^l \left(\frac{2l+1}{l+1}\right)^{l+1} \frac{V^{l+1}}{L^{2l+1}}, \qquad (1)$$

where N_c is the electron density of states, N_t is the total number of trap states per unit volume, μ is the field-independent mobility, e is the charge of electrons, ε_r is the related dielectric constant, ε_0 is the permittivity of free space, L is the thickness of films, and l is defined as the ratio of the characteristic temperature of the trap distribution to the operating temperature. In the low-voltage range of HRS, the conduction is Ohmic (slope: $l+1 \sim 1$), whereas in the high-voltage range of HRS, the current–voltage relationship follows the TL-SCLC mechanism (slope: $l+1 > 1$). Once all the trap sites (e.g., OVs) across the thin film have been connected and filled with the injected electrons, a conducting filamentary path can be created. As a consequence, the current shows a linear dependence on the voltage, indicating Ohmic conduction in LRS. To further elucidate the physical nature of conductive filament in BFMO thin films, the resistances of the LRS for temperatures of 0, 20, 40, 60 °C have been measured, which is demonstrated in the inset of Fig. 3a. As the temperature is increased, the resistance increases slightly. According to the conductive filament mechanism [18, 20], the filament can be created by a large number of OVs, and the formation and rupture of the filament are ascribed to the trapping and detrapping of electrons. When the temperature increases, the detrapping of electrons becomes more convenient, which could weaken the conductive filament, leading to the increase of the resistance.

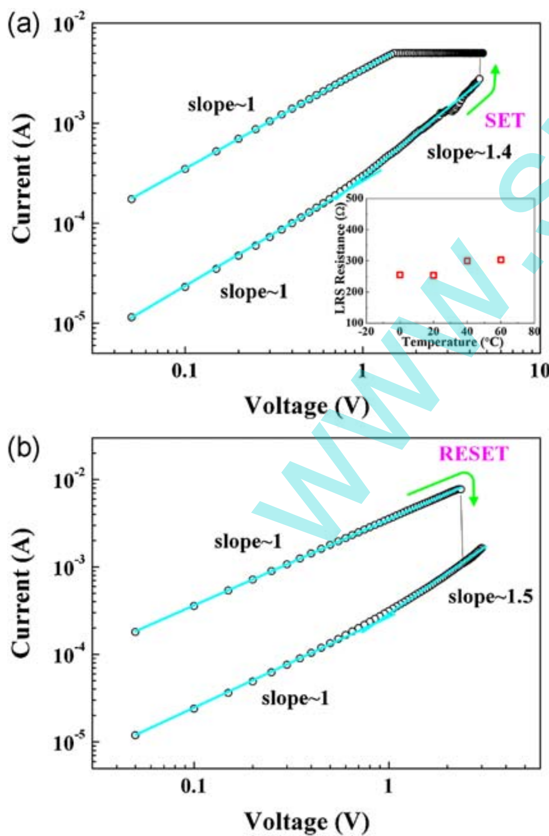

Figure 3 Current–voltage curves of BRS replotted on log–log scale (a) at the positive voltage range and (b) at the negative voltage range. The inset of (a) demonstrates temperature dependence of the LRS resistance with the reading voltage of 0.1 V.

To prevent permanent breakdown, a compliance current is usually necessary during the "SET" process. Figure 4 shows the influence of compliance current on the BRS characteristics in Pt/BFMO/Pt memory devices. The compliance current is varied from 0.1 to 10 mA, and the reproducible resistive switching curves were measured. The switching parameters (the LRS resistance R_L and the RESET current I_R) depending on the compliance current are illustrated in Fig. 4, where the inset shows the corresponding RESET voltage. With increasing the compliance current, the LRS resistance decreases, while the RESET current increases. Accordingly, four resistance levels can be achieved by controlling the compliance current, suggesting that multilevel storage would be feasible. However, to demonstrate this multi-storage capability in detail, more investigation is necessary.

The assumed resistance of filament can be described as

$$R_L = \rho \frac{L}{S}, \qquad (2)$$

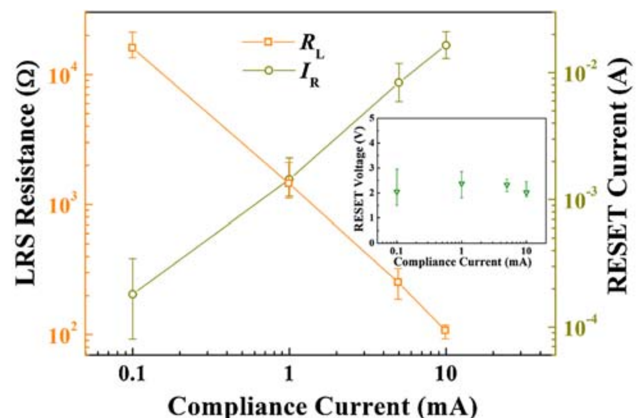

Figure 4 Compliance current effect on the LRS resistance and the RESET current. The inset shows the corresponding RESET voltage.

© 2013 WILEY-VCH Verlag GmbH & Co. KGaA, Weinheim
www.spm.com.cn

where ρ is the filament resistivity and S is the filament area. Considering the power for the detrapping of electrons originates from the substantial Joule heating during the RESET process, the power per unit volume for the detrapping of electrons can be expressed as

$$E = \frac{I_R^2 R_L}{SL}. \tag{3}$$

Combining with Eq. (2), the expression of Eq. (3) is changed to be

$$E = \rho \frac{I_R^2}{S^2} = \frac{1}{\rho L^2} I_R^2 R_L^2 = \frac{1}{\rho L^2} V_R^2, \tag{4}$$

where V_R is the RESET voltage. As we know, larger compliance current can cause the formation of much stronger filaments, leading to the decrease of the LRS resistance [21, 22]. Therefore, to gain enough power to detrap electrons, the lower the LRS resistance becomes, the larger the RESET current will be, just as depicted in Fig. 4. On the other hand, the RESET voltage is found to be independent of the compliance current by Eq. (4), which can be inferred from the inset of Fig. 4. This similar behavior is also reported in other studies [23–25]. Although the properties of a conductive filament can be demonstrated through Eqs. (2)–(4), some values of the parameters (e.g., the filament area) still need to be determined experimentally for further application.

4 Conclusions In summary, Pt/$BiFe_{0.95}Mn_{0.05}O_3$/Pt memory devices with stable bipolar resistive switching characteristics have been fabricated by chemical solution deposition. Based on our previous investigation [18], the conductive-filament mechanism can be used to explain this resistive-switching behavior, which is attributed to the valence change between Fe^{3+} and Fe^{2+} for charge compensation of OVs, corresponding to the trapping and detrapping of electrons. In the present work, the current-conduction studies reveal the importance of oxygen vacancies for the conducting filament formation, and the temperature dependence of the LRS resistance demonstrates the filament electrical property. Moreover, the analysis of the compliance-current effect on the resistive-switching parameters further confirms the applicability of this conductive-filament mechanism.

Acknowledgements The authors greatly thank Prof. B. Wang and Prof. Y. Zheng for valuable suggestions in this work. The authors also gratefully acknowledge the financial support from the NSFC (Nos. 10902128, 10732100, 50802026, 10972239).

References

[1] J. Wang, J. B. Neaton, H. Zheng, V. Nagarajan, S. B. Ogale, B. Liu, D. Viehland, V. Vaithyanathan, D. G. Schlom, U. V. Waghmare, N. A. Spaldin, K. M. Rabe, M. Wuttig, and R. Ramesh, Science **299**, 1719 (2003).
[2] C. Ederer and N. A. Spaldin, Phys. Rev. B **71**, 060401 (2005).
[3] R. Ramesh and N. A. Spaldin, Nature Mater. **6**, 21 (2007).
[4] G. Catalan and J. F. Scott, Adv. Mater. **21**, 2463 (2009).
[5] Y. Zheng, W. J. Chen, X. Luo, B. Wang, and C. H. Woo, Acta Mater. **60**, 1857 (2012).
[6] G. Smolenskii, V. Isupov, A. Agranovskaya, and N. Kranik, Sov. Phys. Solid State **2**, 2651 (1961).
[7] S. V. Kiselev, R. P. Ozerov, and G. S. Zhdanov, Sov. Phys. Dokl. **7**, 742 (1963).
[8] J. Li, J. Wang, M. Wuttig, R. Ramesh, N. Wang, B. Ruette, A. P. Pyatakov, A. K. Zvezdin, and D. Viehland, Appl. Phys. Lett. **84**, 5261 (2004).
[9] Y. P. Wang, L. Zhou, M. F. Zhang, X. Y. Chen, J. M. Liu, and Z. G. Liu, Appl. Phys. Lett. **84**, 1731 (2004).
[10] Y. H. Lee, J. M. Wu, and C. H. Lai, Appl. Phys. Lett. **88**, 042903 (2006).
[11] S. K. Singh, H. Ishiwara, and K. Maruyama, Appl. Phys. Lett. **88**, 262908 (2006).
[12] Y. Shuai, S. Zhou, C. Wu, W. Zhang, D. Bürger, S. Slesazeck, T. Mikolajick, M. Helm, and H. Schmidt, Appl. Phys. Express **4**, 095802 (2011).
[13] X. Chen, G. Wu, H. Zhang, N. Qin, T. Wang, F. Wang, W. Shi, and D. Bao, Appl. Phys. A **100**, 987 (2010).
[14] X. Chen, H. Zhang, K. Ruan, and W. Shi, J. Alloys Compd. **529**, 108 (2012).
[15] C.-H. Yang, J. Seidel, S. Y. Kim, P. B. Rossen, P. Yu, M. Gajek, Y. H. Chu, L. W. Martin, M. B. Holcomb, Q. He, P. Maksymovych, N. Balke, S. V. Kalinin, A. P. Baddorf, S. R. Basu, M. L. Scullin, and R. Ramesh, Nature Mater. **8**, 485 (2009).
[16] K. Yin, M. Li, Y. Liu, C. He, F. Zhuge, B. Chen, W. Lu, X. Pan, and R. W. Li, Appl. Phys. Lett. **97**, 042101 (2010).
[17] X. Zhu, F. Zhuge, M. Li, K. Yin, Y. Liu, Z. Zuo, B. Chen, and R. W. Li, J. Phys. D, Appl. Phys. **44**, 415104 (2011).
[18] J. M. Luo, S. P. Lin, Yue Zheng, and B. Wang, Appl. Phys. Lett. **101**, 062902 (2012).
[19] W. Helfrich and P. Mark, Z. Phys. **166**, 370 (1962).
[20] R. Muenstermann, T. Menke, R. Dittmann, and R. Waser, Adv. Mater. **22**, 4819 (2010).
[21] D. C. Kim, S. Seo, S. E. Ahn, D.-S. Suh, M. J. Lee, B.-H. Park, I. K. Yoo, I. G. Baek, H.-J. Kim, E. K. Yim, J. E. Lee, S. O. Park, H. S. Kim, U.-I. Chung, J. T. Moon, and B. I. Ryu, Appl. Phys. Lett. **88**, 202102 (2006).
[22] C. Rhode, B. J. Choi, D. S. Jeong, S. Choi, J.-S. Zhao, and C. S. Hwang, Appl. Phys. Lett. **86**, 262907 (2005).
[23] W. Guan, S. Long, Q. Liu, M. Liu, and W. Wang, IEEE Electron Device Lett. **29**, 434 (2008).
[24] X. Cao, X. M. Li, X. D. Gao, Y. W. Zhang, X. J. Liu, Q. Wang, and L. D. Chen, Appl. Phys. A **97**, 883 (2009).
[25] Y. Wang, Q. Liu, S. Long, W. Wang, Q. Wang, M. Zhang, S. Zhang, Y. Li, Q. Zuo, J. Yang, and M. Liu, Nanotechnology **21**, 045202 (2010).

www.spm.com.cn

© 2013 WILEY-VCH Verlag GmbH & Co. KGaA, Weinheim